Extended Abstract, 20th Conf. Weather Analysis and Forecasting/
16th Conf. Numerical Weather Prediction
American Meteorological Society, Seattle, Washington, 2004

J5.3 3DVAR Retrieval of 3D Moisture Field from Slant-path Water Vapor Observations of a High-resolution Hypothetical GPS Network

Haixia Liu and Ming Xue

School of Meteorology and Center for Analysis and Prediction of Storms
University of Oklahoma, Norman, Oklahoma

1. Introduction

It is very important to accurately characterize the three-dimensional distribution of water vapor in the atmosphere for the understanding and prediction of mesoscale and storm-scale weather, especially with regard to quantitative precipitation forecasting (Emanuel et al. 1995). Skills in these predictions have been improved rather slowly owing to the high spatial and temporal variability of water vapor. Thus, high resolution observations of three-dimensional water vapor should have capability to improve the prediction of precipitation and severe weather.

In recent years, spaced- and ground-based Global Positioning Systems (GPS) have been developed and become an important instrument that can potentially provide water vapor measurements with high resolution under virtually all weather conditions. Integrated water vapor can be derived from wet signal delay along each slant path between a GPS satellite in view and a ground-based receiver. This water vapor is called slant water vapor with an accuracy of a few millimeters (Braun et al. 2001). Most importantly, slant water vapor can provide vertical structure information of atmospheric moisture.

In the recent years, encouraged by the potential of GPS water vapor sensing, researchers have begun the studies on the impact of GPS water vapor observations on short-range forecasting of convective weather. Kuo et al (1996), Guo et al (2000) and Ha et al (2002), using a 4DVAR system, identified positive impact of assimilating GPS water vapor data into mesoscale models on prediction. MacDonald et al (2002) demonstrated through Observing System Simulation Experiments (OSSE) and 3DVAR (three dimensional variational) analysis that a high-resolution network of GPS receivers can recover the moisture field from the slant integrated water vapor. In their analysis, the integrated slant water vapor measurements are combined with the surface moisture observations assumed to be available at each ground station and with a low density network of water vapor soundings. In their 3DVAR analysis, however, no background moisture field was involved. In order to avoid in the 3DVAR analysis the under-determined problem associated with the number of control variables exceeding the number of observations, approximately 100 GPS observations per surface receiving station were used. This assumes about 100 satellites in view at any particular time, an unrealistic assumption currently and for the near future. Further, a multi-grid analysis procedure was introduced to spread through the injection and interpolation between the two analysis grids observation information in space and to prevent very noisy analysis. In addition, the multi-grid procedure was found necessary to obtain convergence of the cost-function minimization when grid resolution is high (about 10 km).

In this paper, we follow the standard practice of 3DVAR data assimilation for NWP (Lorenc 1981; Daley 1991) by including the analysis background. Consequently, the cost function includes both background and observation terms. The use of a background makes the problem over-determined and the retrieval feasible for experiments using only nine observations per station. Furthermore, the spread of observation in space is achieved in our analysis through background error correlation. In this study, a spatial filter is used to model the background error covariance, and the implementation makes it possible to use flow-dependent anisotropic filters. With the multi-grid technique, it is, difficult, however, to control or tell the amount of spatial smoothing being applied, which affects that spread of observational information therefore the quality of analysis.

We report in the following our work to analyze 3D water vapor distribution from a hypothetical GPS observation network. Sections 2 and 3 describe respectively the GPS measurement principle and our 3DVAR retrieval method. Section 4 describes how we simulate the GPS observation system and obtain mesoscale water vapor distribution using such simulated data, together with the retrieval results. Conclusions and an outline of future work are presented in the final section.

Corresponding Author Address: Dr. Ming Xue,
SOM, 100 E. Boyd, Norman OK 73019,
mxue@ou.edu.

2. GPS Measurement of Slant Water Vapor

The microwave radio signals transmitted by GPS satellites are delayed by the atmosphere as they propagate to the ground-based GPS receivers. The total delay along the slant path is composed of three parts: ionospheric delay, hydrostatic delay and wet delay. Ionospheric delay observed by a dual-frequency GPS receiver can be calculated to millimeter accuracy. The hydrostatic delay can be estimated with the known pressure and temperature. So the wet delay is obtained by subtracting the ionospheric and hydrostatic delays from the total delay. Further, the wet delay due to the presence of water vapor is nearly proportional to the quantity of water vapor integrated along the slant path. Bevis et al (1994) gave the relationship between the slant wet delay (SWD) and the slant water vapor (SWV),

$$SWV = \Pi \bullet SWD \,, \tag{1}$$

where SWV and SWD are given in units of length, and Π is a dimensionless constant, a function of weighted mean temperature of the atmosphere. The accuracy of SWV with this method is about a few millimeters.

3. 3DVAR Retrieval Method

The retrieval method used in this paper is based on 3DVAR method (Lorenc 1981; Daley 1991) which is to minimize the following cost function,

$$\begin{aligned} J(x) &= J_b(x) + J_o(x) \\ &= \frac{1}{2}(x - x_b)^T \mathbf{B}^{-1}(x - x_b) \\ &\quad + \frac{1}{2}\left[H(x) - y\right]^T \mathbf{R}^{-1}\left[H(x) - y\right], \end{aligned} \tag{2}$$

where **B** is the background error covariance which decides how the observation information can be spread in the analysis domain. Since **B** is very large for typical meteorological problems therefore its direct inversion as required by (2) is never attempted. Huang (2000) presented a method named variational analysis using a filter (VAF) which uses the filter to model the effect of **B**. For instance, the following Gaussian filter function can be used to represent **B** for homogeneous and isotropic background error field (Daley 1991) for a three dimensional univariate problem,

$$b_{ij} = \sigma_b^2 \exp\left[-\left(\frac{r_{ij}}{L_r}\right)^2\right], \tag{3}$$

where σ_b^2 is the variance of background error, r_{ij} is the distance between grid point *i* and grid point *j*, and L_r is the length scale decided by the background error correlation and is in practical use sometimes tied to the observation station density. This model represents an isotropic background error covariance. The control variable in the VAF method is the increment field relative to the background rather than the full analysis field itself. Additional details on this method can be found in Huang (2000) and our 3DVAR analysis will be based on this method.

4. Experimental Design

4.1. Observing System Simulation (OSS)

Currently, high-resolution GPS observation network with large spatial coverage does not exist in the United States. Similar to MacDonald et al (2002), we test our analysis system by using simulated data. Experiments as such as commonly referred as Observing System Simulation Experiments and are often used to test the performance of future observing systems. The simulation model is the Advanced Regional Prediction System (ARPS, Xue et al 2000) which is a nonhydrostatic model in a generalized terrain-following coordinate. High-resolution observations from hypothetical GPS networks are created from forecast fields for a dryline case that occurred on June18, 2002 over the Southern Great Plains during the CAPS IHOP real-time forecast period (Xue et al 2002). The 'nature' run is initialized at 1200 UTC June 18, 2002, and is integrated for 3 hours. The computational domain is over the Southern Great Plains with 9 km grid spacing and 53 layers in the vertical.

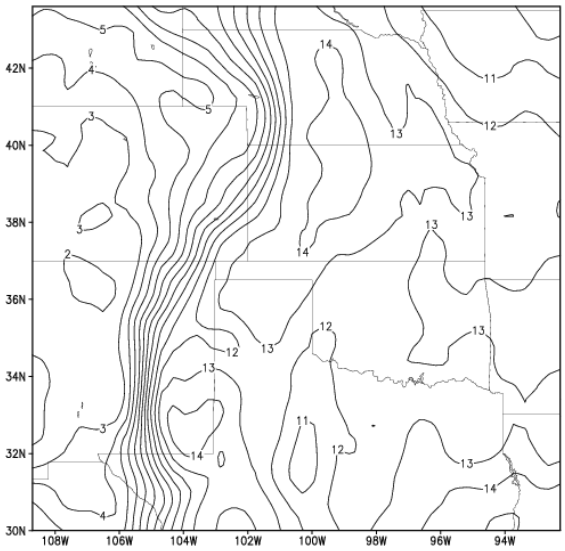

Fig. 1. Specific humidity field (g kg^{-1}) at the second model level (~30m) above ground, valid at 1500 UTC June 18, 2002, from the 'nature' run.

Considering that in the near future, mean spacing of ground receivers of GPS observation networks will probably not be much less than a hundred kilometers, thus the scale of water vapor distribution we can obtain should be of mesoscale. The 9-km 3-hour forecast field, therefore, is thinned by sampling specific humidity every 4 grid points, yielding a resolution of 36 km and a horizontal grid size of 46×41. This gridded field is defined as 'nature' run and used to generate the hypothetical GPS slant water vapor observation data. The specific humidity field at the second model layer (about 30 meters) above ground from the 'nature' run data is presented in Fig.1. A roughly north-south zone of sharp moisture gradient is located to the west of Kansas, Oklahoma and Texas, corresponding to the dryline located in the region. Such strong gradient as well as the variations in strong gradient in water vapor may not be properly captured by ordinary moisture observation networks, especially at levels away from the ground. However, the integrated water vapor along slant paths between surface GPS receivers and satellite can provide three-dimensional information with high temporal and spatial resolutions.

For our OSS experiments, the slant water vapor is obtained by formula,

$$SWV_{ij} = \int_{i^{th}\ receiver}^{j^{th}\ satellite} q\, ds\,, \qquad (4)$$

where ds is the length of elements along slant path, SWV_{ij} the integrated water vapor along the slant path between the i^{th} ground-based GPS receiver and the j^{th} GPS satellite, and q is the specific humidity along the path elements. This value is given by trilinear interpolations from eight surrounding grid points. The hypothetical GPS network is composed of nine irregularly distributed satellites simultaneously in view, and of 132 ground-based receivers which are distributed evenly in the domain. The horizontal resolution of GPS receivers is 144 km so that there is one observation station every 4 points of the 36 km analysis grid. Both sampling and analysis grids are on the ARPS terrain-following coordinate.

4.2. Control Experiment

A control experiment (CNTL) is first performed. In this experiment, two kinds of observation data are used which are the SWV observations from the hypothetical GPS network and the surface regular water vapor observations coincident with ground-based GPS receivers. The receiver sites are commonly equipped with regular meteorological sensors. The analysis background is created by smoothing the 'nature' run 50 times. The control experiment uses 3D Gaussian-type filter with effective filter scales of four grid intervals to simulate the background error covariance. The cost function defined by Eq. (2) is minimized with respect to the increment of specific humidity. Owing to the insignificant effect of the filter on the far distance, the cutoff radii are chosen to be 3 grid intervals in the horizontal and 3 layers in the vertical. The relatively small filter sales and cutoff radii are chosen so that gaps between receiver stations are filled without excessive smoothing to the analysis.

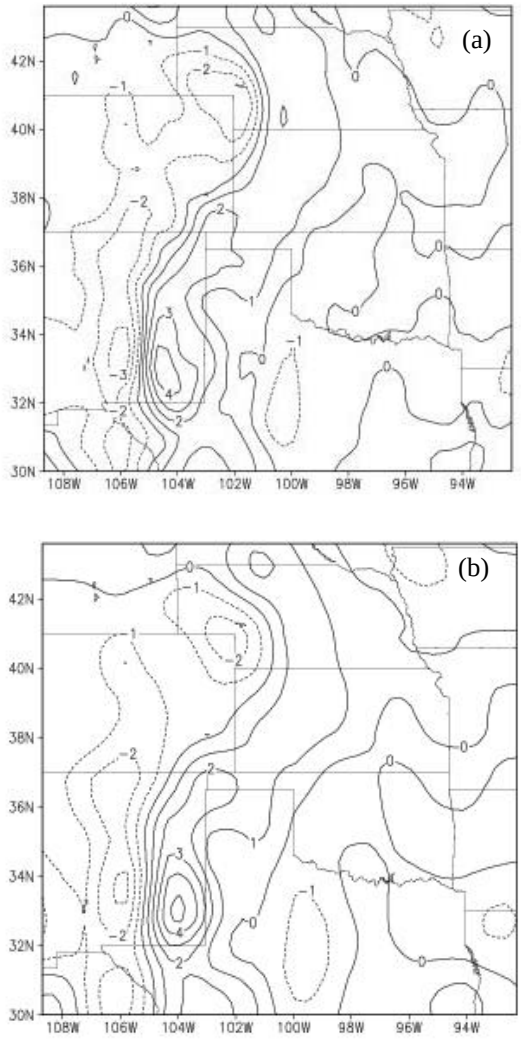

Fig. 2. The increment fields of specific humidity in g kg^{-1} at the second model level (~30m) above ground for (a) the 'nature' run and (b) the control experiment.

With above parameter settings, the control run is conducted. The retrieved moisture field of control run matches well the 'nature' run. Their correlation coefficient for the entire grid is about 0.83. To assess the performance of control experiment, the increment fields,

relative to the background, of the 'nature' and control runs are compared. As an example, their increments at the second model level above ground, are shown in Fig. 2a and 2b, respectively. In Fig. 2a, there is a strong gradient of moisture increment accompanied with maximum and minimum centers located at southeast of New Mexico. This moisture structure is properly recovered by our 3DVAR analysis as shown in Fig. 2b, especially with respect to the relative position of the maximum and minimum centers in the increment field. The retrieved dryline is in the right place.

4.3. Sensitivity Experiments

In order to test the effect of surface moisture observations and vertical filter on the retrieval, two more experiments are conducted.

The first experiment does not include surface observations while other parameter settings are the same as the control experiment. The retrieval result shows that there are only slight differences between this experiment and the control run for moisture distribution above 600 meters AGL. This indicates that the retrieval without surface observations can still capture major features of the 3D moisture field. However, the overall correlation coefficient between retrieval and 'nature' is now 0.69, about 0.14 less than the control run. The decrease in accuracy is mostly due to differences at the lower levels where the surface observations have significant impact. In the absence of surface observations, the low-level background field is little adjusted by the GPS data. This is so since it is the overlapping slant lines in three-dimensional space that provide information for 3D water vapor retrieval. Near the surface, very few slant paths go through the atmosphere due to the relatively high elevation angles of most satellites. The relatively small analysis domain also limits the lowest elevation angle of usable paths.

To determine the effect of vertical filter on the retrieval, only the horizontal filter is used in the second sensitivity experiment, named NVF. All other parameter settings are the same as in the control run. Figure 3 shows the vertical profiles of RMS errors of specific humidity field at horizontal levels from the control and NVF runs. It is clear that the errors of the control run that used vertical filter are smaller than those of NVF. The maximum error for CNTL is about 0.8 k kg^{-1} but 1.2 k kg^{-1} for NVF. There is almost no difference at the surface owing to the use of surface observations. This experiment indicates that without vertical filtering, the retrieved water vapor at the low levels is poor, except at the surface where surface observations are directly available. The reason is again that very few slant paths go through these levels. In the absence of vertical filtering, surface observation information cannot be spread upward to yield a positive effect on the boundary-layer analysis. In conclusion, the vertical filter helps spread observation information in the vertical direction and improves the quality of analysis, especially at the lower levels.

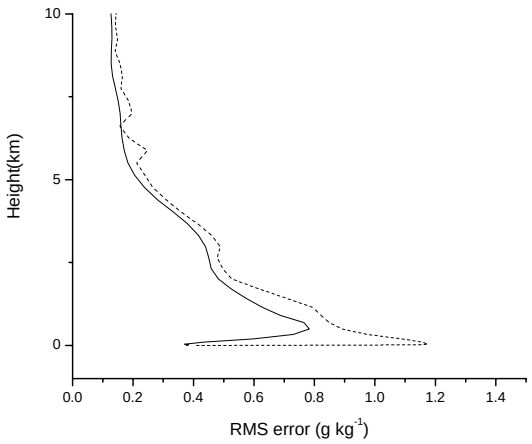

Fig. 3. The RMS error in g kg^{-1} with height. Solid line is for the control run and dashed line for the NVF run.

5. Conclusion and Future Plan

The aim here is to recover three-dimensional water vapor structure from a hypothetic GPS observation network. This network provides integrated water vapor along slant paths between GPS satellites and ground-based receivers and sometimes also direct moisture measurements at the receiver sites. The ARPS mesoscale model is used to produce a "true" atmospheric moisture field, which is used to construct simulated GPS slant-path water vapor data. Three-dimensional variational retrieval experiments are conducted with VAF method. The results illustrate that this variational retrieval method can properly recover mesoscale three-dimensional moisture structure and accurately capture major features of water vapor field simulated by the model in the presence of surface observations. In addition, two sensitivity experiments are conducted to test the effects of surface moisture observations and vertical filter on the retrieval. Results indicate that surface moisture observations are most important for accurate analysis of water vapor field at low levels, where few slant paths pass through. The vertical component of the spatial filter is shown to be very beneficial, especially in data-sparse regions such as the low levels. Otherwise, only the moisture field at middle troposphere can be properly retrieved where enough GPS slant paths overlap. The retrieval in the boundary layer would be improved if more low-elevation angle slant paths were available.

In addition, the use of isotropic background error covariance is based on the assumption that background errors at nearby points are similar. Riishojgaard (1998) points out that the background errors at nearby points that have similar values of the analysis field tend to be similar. Flow-dependent background error covariance based on such an assumption should improve the analysis, especially when data is sparse. This is a topic for future study. Furthermore, we will test the quality of moisture analysis from GPS and other observations by performing forecast experiments using ARPS.

Acknowledgement

This work was supported by NSF grant ATM0129892. The second author was also supported by NSF ATM9909007 and a DOT-FAA grant.

References

Bevis, M., S. Businger, S. Chiswell, 1994: GPS Meteorology: Mapping zenith wet delays onto precipitable water. *J. Appl. Meteor*., **33**, 379-386.

Braun, J., C. Rocken, R. Ware, 2001: Validation of line-of-sight water vapor measurements with GPS. *Radio Sci*., **36**, 459-472.

Daley, R., 1991: *Atmospheric Data Assimilation.* Cambridge University Press, 457 pp.

Emanuel, K., Coauthors, 1995: Report of the first prospectus development team of the U. S. weather research program to NOAA and the NSF. Bull. *Amer. Meteor. Soc.*, **76**, 119-41208.

Guo, Y. R., Y. H. Kuo, J. Dudhia, D. Parsons, 2000: Four-dimensional variational data assimilation of heterogeneous mesoscale observations for a strong convective case. *Mon. Wea. Rev.*, **128**, 619-643.

Ha, S. Y., Y. H. Kuo, Y. R. Guo, G. H. Lim, 2002: Variational assimilation of slant-path wet delay measurements from a hypothetical ground-based GPS network. Part I: Comparison with precipitable water assimilation. *Mon. Wea. Rev.*, submitted.

Huang, X. Y., 2000: Variational analysis using spatial filters. *Mon. Wea. Rev.*, **128**, 2588-2600.

Kuo, Y. H., X. Zou, Y. R. Guo, 1996: Variational assimilation of precipitable water using a nonhydrostatic mesoscale adjoint model. Part I: Moisture retrieval and sensitivity experiments. *Mon. Wea. Rev.*, **124**, 122-147.

Lorenc, A. C., 1981: A global three-dimensional multivariate statistical interpolation scheme. *Mon. Wea. Rev.*, **109,** 701-721.

MacDonald, A. E., Y. Xie, 2002: Diagnosis of three-dimensional water vapor using a GPS network. *Mon. Wea. Rev.*, **130**, 386-397.

Riishojgaard, L. P., 1998: A direct way of specifying flow-dependent background error correlations for meteorological analysis systems. *Tellus*, **50A**, 42-57.

Xue, M., K. K. Droegemeier, and V. Wong, 2000: The Advanced Regional Prediction System (ARPS) - A multiscale nonhydrostatic atmospheric simulation and prediction tool. Part I: Model dynamics and verification. *Meteor. Atmos. Physics*, **75,** 161-193.

Xue, M., K. Brewster, D. Weber, K. W. Thomas, F. Kong, and E. Kemp, 2002: Realtime storm-scale forecast support for IHOP 2002 at CAPS. *Preprint, 15th Conf. Num. Wea. Pred. and 19th Conf. Wea. Aanl. Forecasting*, San Antonio, TX, Amer. Meteor. Soc., 124-126.